Catalysis Science & Technology

Accepted Manuscript

ROYAL SOCIETY OF CHEMISTRY

www.rsc.org/catalysis

Pt-Au/CeO_2 catalysts for the simultaneous removal of carbon monoxide and formaldehyde

Xiaowei Hong[a], Ye Sun[a], Tianle Zhu*[a] and Zhiming Liu*[b]

[a] Beijing Key Laboratory of Bio-inspired Energy Materials and Devices, School of Chemistry and Environment, Beihang University, Beijing 100191, China.

[b] State Key Laboratory of Chemical Resource Engineering, Beijing University of Chemical Technology, Beijing 100029, China.

*Corresponding author: Prof. Tianle Zhu, E-mail: zhutl@buaa.edu.cn; Fax: +86 10 82314215; Tel: +86 10 82314215;

Prof. Zhiming Liu, E-mail: liuzm@mail.buct.edu.cn; Fax: +86 10 64427356; Tel: +86 10 64427356.

Abstract: A series of Pt-Au/CeO_2 catalysts were prepared by impregnation deposition–precipitation (IDP) and reduction-deposition precipitation (RDP) methods. The performances of the catalysts for the simultaneous removal of carbon monoxide (CO) and formaldehyde (HCHO) at room temperature were evaluated. The results showed that Pt-Au/CeO_2 catalyst prepared by the RDP method exhibited higher catalytic activity. The catalyst characterization results revealed that two factors accounted for the phenomenon. The first factor was that more negatively charged metallic Pt nanoparticles were obtained by the liquid phase $NaBH_4$ reduction treatment during preparation process. The second one was that more Au^+ species were formed by using urea as precipitant in Au deposition-precipitation. More of negatively charged metallic Pt nanoparticles and Au^+ species resulted in abundant chemisorbed oxygen, which contributed to the co-oxidation of HCHO and CO. In addition, water exhibited a negative effect on the simultaneous removal of CO and HCHO. Based

upon the results, a possible mechanism for the simultaneous removal of CO and HCHO at room temperature was also proposed.

Keywords: CO; HCHO; Simultaneous removal; Pt-Au/CeO_2; Room temperature

1. Introduction

CO is mainly produced due to the metabolism of human body and HCHO is released from the degradation products of chemical compounds in the apace cabin. Long-term exposure to CO [1] and HCHO [2, 3] can result in detrimental effects on human health and also threaten the safety of humans. Therefore, removal of CO and HCHO has attracted significant attention. For the removal of CO and HCHO, catalytic oxidation is recognized as one of the most effective methods [4].

Recently, a number of efforts have been made to eliminate CO and HCHO at room temperature. Numerous studies related to complete oxidation of HCHO over 1 wt.% Pt/TiO_2 [5], 0.1 wt.% Pt/TiO_2 [6], 0.8 wt.% Pt/AlOOH [7], 1 wt.% Pt/Fe_2O_3 [8] and 1 wt.% Pt/SiO_2 [9] showed that metallic Pt was more active than the oxidized Pt and removal of 100% can be obtained over Pt/TiO_2 at the gas hourly space velocity (GHSV) of 50,000 h^{-1} [5]. For the removal of CO, Au catalysts have been reported to be more active. CO could be oxidized completely at room temperature over 1wt.% Au/TiO_2 [10], 5 wt.% Au/MnO_x [11], 1 wt.% Au/Fe_2O_3 [12], 2.8 wt.% Au/CeO_2 [13], and 2.8 wt.% Au/MOx/CeO_2-Al_2O_3 [14]. And catalytic activity increased with an increase of the amount of cationic Au species for Au catalysts [12, 15, 16].

There exist both HCHO and CO in space cabin. So it is necessary to develop novel catalysts with high activity for the simultaneous removal of HCHO and CO. Since Pt

and Au are active for the individual oxidations of HCHO and CO respectively, a Pt-Au based bimetallic catalyst was naturally proposed. However, CO could be adsorbed on Pt active sites, which makes the bimetallic catalyst prone to being poisoned [17-20]. Such poisoning inhibits the co-oxidization of HCHO and CO as the reaction going on. In our previous study, Pt-Au/TiO_2 bimetallic catalyst with separate Pt and Au active sites presented high catalytic activity for the simultaneous removal of HCHO and CO at the GHSV of 90,000 h^{-1} at room temperature [21]. However, Pt-Au/TiO_2 bimetallic catalyst could not afford the simultaneous removal of HCHO and CO at higher GHSV, whereas small reactor volume is important for space cabin. Therefore, simultaneous removal of HCHO and CO with high activity and stability at relatively higher GHSV at room temperature still remains to be challenging.

The preparation method of catalysts significantly affected their physiochemical properties [15, 21-24]. It was found that reduction treatment enhanced the catalytic activity of Pt catalysts due to affording more metallic Pt [25-27]. Previous research showed that precipitants had a significant influence on the size, dispersion, and chemical states of Au species over catalysts. Urea has been found to be a good precipitant [15, 24]. In addition, CeO_2 was found to be an excellent support for the oxidation of both CO [13, 14] and HCHO [15, 28, 29]. Ordered CeO_2 supported Au catalyst, having higher surface area and better dispersion of active sites, were more active than the disordered CeO_2 supported catalyst [15]. Moreover, nanostructured CeO_2 could enhance the oxygen transfer to active Pt sites [30].

In the present study, Pt-Au/CeO_2 bimetallic catalysts were prepared by the

reduction-deposition precipitation (RDP) (see **Scheme 1**) and impregnation deposition–precipitation (IDP). Physicochemical properties of the Pt-Au/CeO_2 bimetallic catalysts were characterized by N_2 adsorption, high-resolution transmission electron microscopy (HRTEM), temperature programmed reduction by H_2 (H_2-TPR), X-ray photoelectron spectra (XPS), and in-situ Diffuse Reflectance Infrared Fourier Transform Spectroscopy (in-situ DRIFTS). The relationship between the physicochemical properties and the activity for CO and HCHO oxidation of the catalysts has also been discussed.

2. Experimental

2.1. Preparation of the catalysts

The CeO_2 nanospheres were obtained by hydrothermal method. 13 g $Ce(NO_3)_3 \cdot 6H_2O$, 390 mL glycol, 13 mL ultra-pure water and 13 mL propionic acid were added into a teflon-sealed autoclave and then kept at 180 ℃ for 10 h. After hydrothermal treatment, the suspension was centrifuged and washed with ultra-pure water. The precipitate was dried at 100 ℃ for 12 h and then calcined in air at 400 ℃ for 4 h to get the CeO_2 nanospheres.

The Pt-Au/CeO_2 (IDP) catalyst was prepared by the impregnation deposition–precipitation (IDP) method [21]. 4 g CeO_2 was added to 40 mL H_2PtCl_6 solution containing 0.04 g Pt and was stirred for 2 h. Water was removed by rotary evaporator under vacuum at 60℃ and the precipitate was dried at 80 ℃ for 12 h. Pt/CeO_2 was obtained after the solid was calcined at 400 ℃ for 4 h in air. The pH value of the Pt/CeO_2 suspension was adjusted to 9-10 by using aqueous NaOH solution. 10 mL

$HAuCl_4$ solution containing 0.02 g Au was added to this suspension and was vigorously stirred for 2 h. After the suspension was aged at 75 ℃ for 2 h, the suspension was filtered and washed with ultra-pure water. Then the solid was dried under vacuum at 80 ℃ for 12 h. Subsequently, Pt-Au/CeO_2 (IDP) catalyst was obtained after the precipitate was calcined at 200 °C in air for 4 h.

Pt-Au/CeO_2 (RDP) catalyst was acquired by reduction-deposition precipitation (RDP) method. 4 g CeO_2 was uniformly dispersed into the H_2PtCl_6 solution containing 0.04 g Pt and was stirred for 2 h. After adjusting the pH value of the suspension to 10 by using aqueous NaOH solution, $NaBH_4$ (molar ratio of $NaBH_4$ to Pt=10) solution was quickly added to the suspension. The solution was continuously stirred for 2 h. The suspension was filtered and washed with ultra-pure water. It was dried under vacuum at 120 °C for 12 h to obtain Pt/CeO_2. Urea solution (molar ratio of urea to Au=125) and 2 g Pt/CeO_2 were uniformly dispersed into the $HAuCl_4$ solution containing 0.02 g Au. The solution was stirred at 80 °C for 8 h. After the suspension was aged for 12 h at room temperature, it was filtered and the precipitant was washed with ultra-pure water. The solid was dried at room temperature under vacuum for 12 h to obtain Pt-Au/CeO_2 (RDP) catalyst.

2.2. Characterization of the catalysts

Surface areas of the catalysts were determined according to the BET method by using a Micromeritics' ASAP 2000 instrument. HRTEM micrographs were obtained with a JEM-2100F microscope at 200 kV. The surface chemical states of Pt-Au/CeO_2 catalysts were investigated by XPS (PHI Quantro SXM ULVAC-PHI, Japan) using an

Al Kα X-ray source (1486.7 eV) at 15 kV and 25 W with the binding energy calibrated by C 1s at 284.8 eV.

In-situ DRIFTS spectra were obtained in a Nicolet 6700 FTIR spectrometer. Before the experiments, all the catalysts were pretreated with Ar at 100 °C for 1 h. After being cooled to 25 °C, the reactant gas, containing 100 ppm HCHO, 800 ppm CO and synthetic air at 100 mL·min^{-1}, was introduced into the DRIFT cell. All spectra were recorded by accumulating 32 scans with a resolution of 4 cm^{-1}. H_2-TPR measurements were carried out in a fixed bed microreactor, which was equipped with a quadrupole mass spectrometer (Omnistar, GSD-301-O_2). 0.2 g sample was pretreated under Ar at 100 °C for 1 h. After being cooled to 25 °C, the catalyst was reduced by 5% H_2/N_2 at 50 mL·min^{-1} in the temperature range of 30 to 350 °C with a heating rate of 10 °C·min^{-1}. Prior to the characterization, the pretreatments were performed as follows: fresh Pt-Au/CeO_2 (IDP) catalyst was pretreated by 5% H_2/N_2 at 100 mL·min^{-1} at 200 °C for 1 h, while the Pt-Au/CeO_2 (RDP) fresh catalyst was pretreated with Ar at 100 °C for 1 h. Pt^0 species are more active than Pt^{2+} species for the oxidation of HCHO, so reduction treatment for the catalyst (IDP) is necessary. For the catalyst (RDP), it is not necessary for H_2 pretreatment because the Pt species have already been reduced by $NaBH_4$.

2.3. Measurement of the catalytic activities

Activity evaluation for the simultaneous removal of CO and HCHO was carried out by using 0.36 g catalyst at 25 °C. Before evaluating the activity, Pt-Au/CeO_2 (IDP) catalyst was pretreated at 200 °C by 5% H_2/N_2 at 100 mL·min^{-1} for 1 h, while

Pt-Au/CeO_2 (RDP) catalyst was pretreated at 100 °C by Ar at 100 mL·min^{-1} for 1 h. After the catalyst was cooled to 25 °C, the reaction gas, comprising of 100 ppm CO, 50 ppm HCHO and air with 50% relative humidity (RH), was introduced to the reactor at a rate of 1800 mL·min^{-1} (which corresponds to a GHSV of 250,000 h^{-1}). CO and CO_2 were detected by a gas chromatograph (GC) equipped with CH_4 converter, while HCHO was analyzed by an acetylacetone-based spectrophotometric method.

3. Results and discussion

3.1. Catalytic activities of the catalysts

Fig. 1 presents the activities of the Pt-Au/CeO_2 catalysts for the catalytic co-oxidation of CO and HCHO. 97% conversion of CO and 80% conversion of HCHO are observed over Pt-Au/CeO_2 (IDP) catalyst. It is worth noting that the conversions of both CO and HCHO gradually decrease, which can be attributed that CO cannot completely be removed from Au active sites, resulting in CO accumulation on Au active sites and CO self-poisoning over Pt active sites [20, 21, 31]. In contrast, 100% conversions of CO and HCHO are obtained for Pt-Au/CeO_2 (RDP) catalyst. More importantly, it shows high stability, which is very important for the practical applications.

Fig. 2 shows the effect of Au content on the catalytic performance of Pt-Au/CeO_2 (RDP) catalyst with Pt content of 1 wt.%. Conversions of CO and HCHO increase with increasing Au content. This is due to the reason that more Au species enhance the removal of CO and decrease the CO poisoning effect on the Pt active sites. When Au content is 1 wt.%, CO and HCHO conversion of 100% can obtained. Therefore, the

optimized Au content is 1 wt.% for a 1 wt.% Pt content in the catalyst. The effect of RH on the catalytic performance of Pt-Au/CeO_2 (RDP) catalyst was investigated after the catalyst was exposed to 100 ppm CO + 50 ppm HCHO + Synthetic air at the GHSV of 250,000 h^{-1} for 60 min and the results were presented in **Fig. 3**. It can be seen that the catalytic activity decreases with the increase of RH. This is attributed to that the accumulation of water occupied the Pt and Au active sites [32] at relatively high RH and thus, hinder the co-oxidation of CO and HCHO.

3.2. Physicochemical properties of the catalysts

Pore size distributions of CeO_2 nanospheres are shown in **Fig. 4**. It shows that CeO_2 nanospheres' pore size is mainly distributed near 2 nm and 5 nm. BET surface area and pore volume results for CeO_2 nanospheres and Pt-Au/CeO_2 catalysts are presented in **Table 1**. The results show that CeO_2 nanospheres have high surface area (184.3 $m^2 \cdot g^{-1}$). In addition, the decrease of surface areas of Pt-Au/CeO_2 catalysts is due to the deposition of Pt and Au nanoparticles on CeO_2 nanospheres. Values for the dispersion of metal on catalyst (IDP) and catalyst (RDP) are 51.7% and 62.3% respectively. This indicates that the RDP method affords a higher dispersion. It can be seen that many CeO_2 crystallite particles constitute the CeO_2 nanospheres, which have a diameter in the range of 70-100 nm (as shown in **Fig. 5a)**. Moreover, BET results show significant voids. **Fig. 5b** shows that CeO_2 nanospheres present (111) plane based on the FFT results, which is the same as the result of Ma et al. [33]. **Fig. 5c** and **Fig. 5d** present the EDX spectra for Pt-Au/CeO_2 (IDP) and Pt-Au/CeO_2 (RDP) catalysts respectively. The content of Pt and Au in Pt-Au/CeO_2 (IDP) catalyst and

Pt-Au/CeO_2 (RDP) catalyst are close to the theoretical value (1 wt.%), which suggests that both of the preparation methods can afford a low loss of Pt and Au species. Compared to the XPS results presented in **Table 1**, the contents of Pt and Au in Pt-Au/CeO_2 (IDP) catalyst are close to the EDX results, indicating that Pt and Au are mainly distributed on the outer surface of the CeO_2 nanospheres. However, the contents of Pt and Au in Pt-Au/CeO_2 (RDP) catalyst are less than the EDX results, suggesting that most of Pt and Au are well distributed on the inner surface of CeO_2 nanospheres. The quantity of surface Au species and Pt species on Pt-Au/CeO_2 (RDP) catalyst are smaller than that on Pt-Au/CeO_2 (IDP) catalyst, however the dispersion of Au species and Pt species on Pt-Au/CeO_2 (RDP) catalyst are higher than that on Pt-Au/CeO_2 (IDP) catalyst. Different dispersion methods of Pt and Au species on Pt-Au/CeO_2 catalyst may cause the significant decrease in the specific surface area.

The H_2-TPR profiles of the CeO_2 nanospheres and Pt-Au/CeO_2 catalysts are presented in **Fig. 6**. Pure CeO_2 shows no reduction peak at 20-350 °C [34]. For the Pt-Au/CeO_2 (IDP) catalyst, there are three reduction peaks at 72, 149 and 218 °C. The Au reduction of Au/CeO_2 catalyst occurs at 100-200 °C [15, 35]. So, the reduction peak at 149 °C is ascribed to Au reduction, while the reduction peaks at 72 and 218 °C are assigned to surface oxygen reduction of CeO_2 and Pt reduction respectively [36]. Hydrogen consumption is much more than that needed for the reduction of PtO_x at 72 °C, indicating that most of the hydrogen is consumed by CeO_2 contacting with Pt, which happened due to the hydrogen spillover from Pt species to CeO_2 [8, 36]. For the Pt-Au/CeO_2 (RDP) catalyst, there is no Pt reduction peak,

indicating that cationic Pt is reduced to metallic Pt by $NaBH_4$. Compared to cationic Pt, metallic Pt is much more active for absorbing and converting HCHO species to formate by enhancing oxygen activation [6, 25]. Therefore, Pt-Au/CeO_2 (RDP) is more active than Pt-Au/CeO_2 (IDP) for HCHO oxidation. The reduction peak at 125 °C is ascribed to Au reduction peak in Pt-Au/CeO_2 (RDP) catalyst. Reduction temperature Pt-Au/CeO_2 (RDP) is lower than that of Pt-Au/CeO_2 (IDP).The acceleration of Au-reduction could be due to the hydrogen dissociation on metal-Pt.

To investigate the chemical states of the Pt and Au species on the activity of catalysts, XPS characteristics for fresh Pt-Au/CeO_2 catalyst were carried out, as shown in **Fig. 7** and in **Table 2**. The Pt 4f includes Pt $4f_{7/2}$ and Pt $4f_{5/2}$ and Pt $4f_{7/2}$ is usually investigated to evaluate the activity of Pt catalyst. The BE values of Pt $4f_{7/2}$ at 70.7 and 72.4 are ascribed to Pt^0 and Pt^{2+} respectively, suggesting that there are two chemical states in the Pt-Au/CeO_2 (IDP) (**Fig. 7a)** [37]. The Au 4f includes Au $4f_{7/2}$ and Au $4f_{5/2}$, and Au $4f_{7/2}$ is investigated to evaluate the activity of Au catalyst. For Pt-Au/CeO_2 (IDP) catalyst, the BE values of Au $4f_{7/2}$ at 83.6 eV and 84.5 eV are assigned to Au^0 and Au^+ respectively (**Fig. 7b)** [38]. **Fig. 7c** shows that the BE of Pt $4f_{7/2}$ at 70.7 eV corresponds to Pt^0 in the Pt-Au/CeO_2 (RDP) catalyst and there is no peaks assigned to Pt^{2+}, indicating that the cationic Pt is reduced to metallic Pt. **Fig. 7d** shows a signal at the BE of 84.2 eV, which is assigned to Au^+ in the Pt-Au/CeO_2 (RDP) catalyst, and there is no peak assigned to Au^0.

Based on the XPS results, the ratios of both Pt^0 to the total surface Pt (Pt^0 and Pt^{2+}) and that of Au^+ to the total surface Au (Au^0 and Au^+) are calculated (see **Table 2**). The

BE of metallic Pt (Pt^0) appears to be negatively shifted from 71.1 eV to 70.7 eV in Pt-Au/CeO_2 (IDP) and Pt-Au/CeO_2 (RDP) catalysts due to the charge transfer, which enhances the activation of oxygen [6]. The amount of negatively charged metallic Pt in Pt-Au/CeO_2 (RDP) catalyst is more than that in Pt-Au/CeO_2 (IDP) catalyst, leading to a higher catalytic activity for HCHO oxidation [25]. The cationic Au can more easily adsorb O_2 than Au^0 and thus, possesses higher activity for CO oxidation, which has been verified in the previous report [10, 16, 39-41]. In addition, Au^+ carbonyls are the most stable gold carbonyls in the form of Au^+-CO species [16, 42, 43]. The amount of Au^+ in Pt-Au/CeO_2 (RDP) catalyst is five times higher than that in Pt-Au/CeO_2 (IDP) catalyst, indicating that Pt-Au/CeO_2 (RDP) catalyst can afford higher catalytic activity for CO oxidation.

To study the chemical states of oxygen in fresh samples, O1s XPS spectra are studied，as shown in **Fig. 8** and **Table 3**. The O1s XPS spectra show two peaks at 529.3 and 531.3 eV. The former is ascribed to lattice oxygen (O_I) and the latter is attributed to the oxygen (O_{II}) chemisorbed on the surface [6]. It is apparent that the $O_{II}/(O_{II}+O_I)$ ratio over Pt-Au/CeO_2 (RDP) is much higher than that over Pt-Au/CeO_2(IDP)(48% vs 19%), which suggests that both the negatively charged metallic Pt and Au^+ enhance the capacity of O_2 adsorption and the absorbed O_2 is also activated during the charge transfer [44-46]. A larger quantity of oxygen, chemisorbed on the surface, is beneficial to activate the HCHO and CO, which facilitates the catalytic oxidation reaction [6, 42, 43, 47]. Therefore, the abundant chemisorbed oxygen is mainly responsible for the high activity of Pt-Au/CeO_2 (RDP) catalyst for

247 the co-oxidation of HCHO and CO.

248 Based upon the XPS results, it can be seen that Pt^0 species can be obtained after
249 the H_2 treatment for Pt-Au/CeO_2 (IDP) catalyst. However, The RDP method could
250 provide more Pt^0 species than that of IDP method, due to the reduction by $NaBH_4$.
251 During the deposition-precipitation of Au species, urea, which is used as a precipitant,
252 could afford more cationic Au species than that of NaOH. This is due to the reason
253 that urea affords the gradual and homogeneous addition of hydroxide ions throughout
254 the whole solution, which helps avoid local increase in pH and the precipitation of
255 metal hydroxide in the solution. The reaction of urea in water can be presented as:

256 $$CO(NH_2)_2 + 3H_2O \rightarrow 2NH_4^+ + CO_2 + 2OH^-$$

257 To further investigate the relationship between the catalyst activity and the
258 catalyst physicochemical properties, in-situ DRIFT spectra of the Pt-Au/CeO_2
259 catalysts obtained upon exposure to CO, HCHO and synthetic air at 25 ^oC are shown
260 in **Fig. 9**. The peaks at 1580-1575 cm^{-1} and 1365-1361 cm^{-1} are ascribed to
261 antisymmetrical and symmetrical stretching bands of formate [15, 21, 35]. The peak
262 at 2080-1856 cm^{-1} is ascribed to CO species adsorbed on Pt sites [48], while the peak
263 at 2160-2107 cm^{-1} is assigned to CO species adsorbed on Au sites [49, 50]. HCHO can
264 be oxidized over two kinds of Pt-Au/CeO_2 catalysts because no peaks, ascribed to
265 HCHO, are detected in **Fig. 9a** and **9c**. The intensity of the peak at 1575 cm^{-1}
266 gradually increases, indicating that high concentration CO is mainly chemisorbed and
267 oxidized on Au sites, while HCHO is oxidized on Pt active sites. The intensity of the
268 peak at 1575 cm^{-1} (0.38 km) on Pt-Au/CeO_2 (RDP) catalyst is higher than that (0.3 km)

on Pt-Au/CeO_2(IDP) catalyst, indicating that more HCHO is absorbed and oxidized on Pt sites over Pt-Au/CeO_2 (RDP) catalyst, which is in accordance with the XPS result. **Fig. 9b** presents two peaks at 2127 and 2016 cm^{-1} ascribed to CO species adsorbed on Au and Pt sites in Pt-Au/CeO_2 (IDP) catalyst. However, the peaks at 2160 cm^{-1} and 2080 cm^{-1} are ascribed to CO species adsorbed on Au and Pt sites in Pt-Au/CeO_2 (RDP) catalyst. It is obvious that the red shift appears on the peaks of CO species adsorbed on Au and Pt sites on Pt-Au/CeO_2 (RDP) catalyst, indicating that the intermediate O_2-Au^+-CO is more stable [50, 51], which contributes to the CO oxidation. In addition, the accumulated amount of CO on Pt-Au/CeO_2 (RDP) catalyst is less than that on the Pt-Au/CeO_2 (IDP) catalyst, suggesting that more cationic Au active sites promote the oxidation of CO. Previous research has shown that cationic Au plays a crucial role in catalyzing CO oxidation over Au catalysts [10, 16, 52].

Previous researches have proposed that the mechanism of HCHO oxidation over Pt catalysts is that HCHO is absorbed, oxidized into formate and then decomposed into CO_2 and H_2O, successively [53]. And oxygen was first absorbed on the surface of the catalyst and then acted as the active centers for HCHO oxidation[6]. A number of mechanisms have been proposed for CO oxidation on Au catalyst. A widely accepted mechanism is that CO is adsorbed on metallic Au sites in the form of O_2-Au^+-CO as intermediates for CO oxidation [11]. Base on the mechanism for individual oxidation of CO and HCHO, one possible mechanism for the co-oxidation of CO and HCHO, has been proposed (see **Fig. 10**). As shown in **Fig. 10**, two kinds of intermediate are supposed to be formed on Pt-Au/CeO_2 catalyst and the chemisorbed oxygen (O_{II})

plays an important role in the co-oxidation of CO and HCHO.

Conclusions

The present research shows that Pt-Au/CeO_2 catalyst prepared by reduction-deposition precipitation method presents high activity for the simultaneous removal of HCHO and CO at room temperature. Over this catalyst, more negatively charged metallic Pt and Au^+ could enhance the electron transfer, activation and the mobility of oxygen species, resulting in formation of more chemisorbed oxygen (O_{II}). The abundant chemisorbed oxygen (O_{II}) is mainly responsible for the higher activity of Pt-Au/CeO_2 (RDP) catalyst for the simultaneous removal of CO and HCHO. In addition, the catalytic activity decreases with an increase of RH. The results obtained in this study elaborate the possibility of the simultaneous removal of HCHO and CO at relatively high GHSV.

Acknowledgments

This work has been financially supported by Special Foundation for Environmental Public Sector Research of Ministry of Environmental Protection of People's Republic of China (No. 201409080).

References

[1] P.W. Seo, H.J. Choi, S.I. Hong, S.C. Hong, J. Hazard. Mater., 2010, 178, 917.
[2] L.F. Wang, M. Sakurai, H. Kameyama, J. Hazard. Mater., 2009, 167, 399.
[3] J.G. Yu, X.Y. Li, Z.H. Xu, W. Xiao, Environ. Sci. Technol., 2013, 47, 9928.
[4] X.F. Tang, J.L. Chen, X.M. Huang, Y. Xu, W.J. Shen, Appl. Catal. B, 2008, 81, 115.
[5] C.B. Zhang, H. He, K. Tanaka, Appl. Catal. B, 2006, 65, 37.
[6] H. Huang, D.Y.C. Leung, D. Ye, J. Mater. Chem., 2011, 21, 9647.
[7] Z.H. Xu, J.G. Yu, M. Jaroniec, Appl. Catal. B, 2015, 163, 306.
[8] N.H. An, Q.S. Yu, G. Liu, S.Y. Li, M.J. Jia, W.X. Zhang, J. Hazard. Mater., 2011, 186, 1392.
[9] N.H. An, W.L. Zhang, X.L. Yuan, B. Pan, G. Liu, M.J. Jia, W.F. Yan, W.X. Zhang, Chem. Eng. J., 2013, 215, 1.
[10] J. Yu, G.S. Wu, G.Z. Lu, D.S. Mao, Y. Guo, RSC Adv., 2014, 4, 16985.

[11] L.C. Wang, X.S. Huang, Q. Liu, Y.M. Liu, Y. Cao, H.Y. He, K.N. Fan, J.H. Zhuang, J. Catal., 2008, 259, 66.
[12] B. Qiao, J. Zhang, L. Liu, Y. Deng, Appl. Catal. A, 2008, 340, 220.
[13] S. Carrettin, P. Concepcion, A. Corma, J.M. Lopez Nieto, V.F. Puntes, Angew. Chem. Int. Ed., 2004, 43, 2538.
[14] T.R. Reina, A.A. Moreno, S. Ivanova, J.A. Odriozola, M.A. Centeno, Chemcatchem, 2012, 4, 512.
[15] B.B. Chen, C.A. Shi, M. Crocker, Y. Wang, A.M. Zhu, Appl. Catal. B, 2013, 132, 245.
[16] G. Hutchings, M. Hall, A. Carley, P. Landon, B. Solsona, C. Kiely, A. Herzing, M. Makkee, J. Moulijn, A. Overweg, J. Catal., 2006, 242, 71.
[17] T. Schmidt, Z. Jusys, H. Gasteiger, R. Behm, U. Endruschat, H. Boennemann, J. Electroanal. Chem., 2001, 501, 132.
[18] H. Zhang, X. Liu, N. Zhang, J. Zheng, Y. Zheng, Y. Li, C.-J. Zhong, B.H. Chen, Appl. Catal. B, 2016, 180, 237.
[19] J. Ayastuy, M. Gonzalez-Marcos, J. Gonzalez-Velasco, M. Gutierrez-Ortiz, Appl. Catal. B, 2007, 70, 532.
[20] G. Avgouropoulos, T. Ioannides, Appl. Catal. B, 2005, 56, 77.
[21] H.B. Na, T. Zhu, Z.M. Liu, Catal. Sci. Technol., 2014, 4, 2051.
[22] A.M. Da Silva, K.R. De Souza, G. Jacobs, U.M. Graham, B.H. Davis, L.V. Mattos, F.B. Noronha, Appl. Catal. B, 2011, 102, 94.
[23] X. Li, P. Liu, Y. Mao, M. Xing, J. Zhang, Appl. Catal. B, 2015, 164, 352.
[24] R. Zanella, S. Giorgio, C.R. Henry, C. Louis, J. Phys. Chem. B, 2002, 106, 7634.
[25] Z.H. Li, K. Yang, G. Liu, G.F. Deng, J.Q. Li, G. Li, R.L. Yue, J. Yang, Y.F. Chen, Catal. Lett., 2014, 144, 1080.
[26] H.B. Huang, D.Y.C. Leung, D.Q. Ye, J. Mater. Chem., 2011, 21, 9647.
[27] O.S. Alexeev, S.Y. Chin, M.H. Engelhard, L. Ortiz-Soto, M.D. Amiridis, J. Phys. Chem. B, 2005, 109, 23430.
[28] G. Li, L. Li, RSC Adv., 2015, 5, 36428.
[29] Q.L. Xu, W.Y. Lei, X.Y. Li, X.Y. Qi, J.G. Yu, G. Liu, J.L. Wang, P.Y. Zhang, Environ. Sci. Technol., 2014, 48, 9702.
[30] G.N. Vayssilov, Y. Lykhach, A. Migani, T. Staudt, G.P. Petrova, N. Tsud, T. Skála, A. Bruix, F. Illas, K.C. Prince, Nat. Mater., 2011, 10, 310.
[31] L.Q. Liu, B.T. Qiao, Y.D. He, F. Zhou, B.Q. Yang, Y.Q. Deng, J. Catal., 2012, 294, 29.
[32] I.X. Green, W. Tang, M. Neurock, J.T. Yates, Angew. Chem. Int. Ed., 2011, 50, 10186.
[33] L. Ma, D.S. Wang, J.H. Li, B.Y. Bai, L.X. Fu, Y.D. Li, Applied Catalysis B-Environmental, 2014, 148, 36.
[34] X. Cheng, A. Zhu, Y. Zhang, Y. Wang, C.T. Au, C. Shi, Appl. Catal. B, 2009, 90, 395.
[35] H.F. Li, N. Zhang, P. Chen, M.F. Luo, J.Q. Lu, Appl. Catal. B, 2011, 110, 279.
[36] I.D. Gonzalez, R.M. Navarro, W. Wen, N. Marinkovic, J.A. Rodriguez, F. Rosa, J.L.G. Fierro, Catal. Today, 2010, 149, 372.
[37] M.J. Tiernan, O.E. Finlayson, Appl. Catal. B, 1998, 19, 23.
[38] Q. Fu, H. Saltsburg, M. Flytzani-Stephanopoulos, Science, 2003, 301, 935.
[39] G.C. Bond, D.T. Thompson, Gold Bull., 2000, 33, 41.
[40] J. Guzman, B.C. Gates, J. Am. Chem. Soc., 2004, 126, 2672.
[41] B. Yoon, H. Häkkinen, U. Landman, A.S. Wörz, J.-M. Antonietti, S. Abbet, K. Judai, U. Heiz, Science,

2005, 307, 403.
[42] F.M. S. Arrii, A. J. Renouprez, and J. L. Rousset, J. Am. Chem. Soc., 2004, 126, 1199.
[43] G.J. Hutchings, Dalton Trans., 2008, 5523.
[44] J.A. van Bokhoven, C. Louis, J.T. Miller, M. Tromp, O.V. Safonova, P. Glatzel, Angew. Chem. Int. Ed., 2006, 45, 4651.
[45] T. Jacob, B.V. Merinov, W.A. Goddard, Chem. Phys. Lett., 2004, 385, 374.
[46] A.P. Farkas, T. Diemant, J. Bansmann, R.J. Behm, Chemphyschem, 2012, 13, 3516.
[47] L. Ma, D.S. Wang, J.H. Li, B.Y. Bai, L.X. Fu, Y.D. Li, Appl. Catal. B, 2014, 148, 36.
[48] H.N. Evin, G. Jacobs, J. Ruiz-Martinez, U.M. Graham, A. Dozier, G. Thomas, B.H. Davis, Catal. Lett., 2007, 122, 9.
[49] A. Chiorino, M. Manzoli, F. Menegazzo, M. Signoretto, F. Vindigni, F. Pinna, F. Boccuzzi, J. Catal., 2009, 262, 169.
[50] M. Comotti, W.-C. Li, B. Spliethoff, F. SchÜth, J. Am. Chem. Soc., 2006, 917.
[51] F. Boccuzzi, A. Chiorino, J. Phys. Chem. B, 2000, 104, 5414.
[52] A. Karpenko, R. Leppelt, J. Cai, V. Plzak, A. Chuvilin, U. Kaiser, R.J. Behm, J. Catal., 2007, 250, 139.
[53] C. Zhang, H. He, Catal. Today, 2007, 126, 345.

Table 1: Textural porosities and chemical compositions of Pt-Au/CeO_2 catalysts

Sample	S_{BET} ($m^2\ g^{-1}$)	Dispersion [a] (%)	Pore Volume ($cm^3 g^{-1}$)	Surface composition [b] (wt.%)	
				Pt	Au
CeO_2 nanospheres	184.3	–	0.34	–	–
Pt-Au/CeO_2 (IDP)	175.1	51.7	0.34	0.68	0.73
Pt-Au/CeO_2 (RDP)	156.4	62.3	0.33	0.35	0.31

[a] Metal dispersion determined by CO-chemisorption. [b] Surface composition determined by XPS.

Table 2: Analysis of XPS data for Pt-Au/CeO_2 catalysts

Catalyst	Peak position (eV)		Content (at.%)	Peak position (eV)		Content (at.%)
	Pt^0	Pt^{2+}	Pt^0/Pt^0+Pt^{2+}	Au^0	Au^+	Au^+/Au^0+Au^+
Pt-Au/CeO_2(IDP)	70.7	72.4	75	83.6	84.5	18
Pt-Au/CeO_2(RDP)	70.7	—	100	—	84.2	100

Table 3: O1s XPS data for different Pt-Au/CeO_2 catalysts

Catalysts	Peak position (eV)		Surface atomic ratio
	O_{II}	O_I	O_{II} / O_{II}+ O_I
Pt-Au/CeO_2(IDP)	531.8	529.5	19
Pt-Au/CeO_2(RDP)	531.4	529.2	48

Scheme 1: Schematic illustration of the procedure for the preparation of Pt-Au/CeO_2 (RDP) catalyst.

Figure 1: Activities of Pt-Au/CeO_2 (IDP) and Pt-Au/CeO_2 (RDP) catalysts for catalytic co-oxidation of HCHO and CO. Reaction conditions: 50 ppm HCHO/100 ppm CO/air (50% relative humidity); temperature: 25 $^{\circ}$C; GHSV = 250,000 h^{-1}.

Figure 2: Effect of Au content on the catalytic activity of Pt-Au/CeO_2 (RDP) catalyst for the co-oxidation of CO and HCHO.

Figure 3: Effect of RH on the catalytic activity of Pt-Au/CeO_2 (RDP) catalyst for the co-oxidation of CO and HCHO.

Figure 4: (a) N_2 adsorption and desorption isotherms for CeO_2 nanospheres. (b) BJH pore size distribution curves for CeO_2 nanospheres.

Figure 5: (a) **TEM** images of CeO_2 nanosphere. (b) **HRTEM** images of CeO_2 nanosphere (Bottom-right inset shows the corresponding FFT pattern). (c)**TEM** images and **EDX** spectra of Pt-Au/CeO_2 (IDP) catalyst. (d) **TEM** images and **EDX** spectra of Pt-Au/CeO_2 (RDP) catalyst.

Figure 6 : H_2-TPR profiles of Pt-Au/CeO_2 catalysts. (a) Pt-Au/CeO_2 (RDP). (b) Pt-Au/CeO_2 (IDP). (c) CeO_2 nanospheres.

Figure 7: Pt 4f and Au 4f XPS spectra of Pt-Au/CeO_2 catalysts.

Figure 8: O1s XPS spectra of different Pt-Au/CeO_2 catalysts.

Figure 9: In-situ DRIFTS of the Pt-Au/CeO_2 catalysts after being exposed to 800 ppm CO + 100 ppm HCHO + Synthetic air at 25 °C. (a) and (b): Pt-Au/CeO_2 (IDP) catalyst. (c) and (d): Pt-Au/CeO_2 (RDP) catalyst.

Figure 10: A proposed mechanism for the catalytic co-oxidation of CO and HCHO

Scheme 1

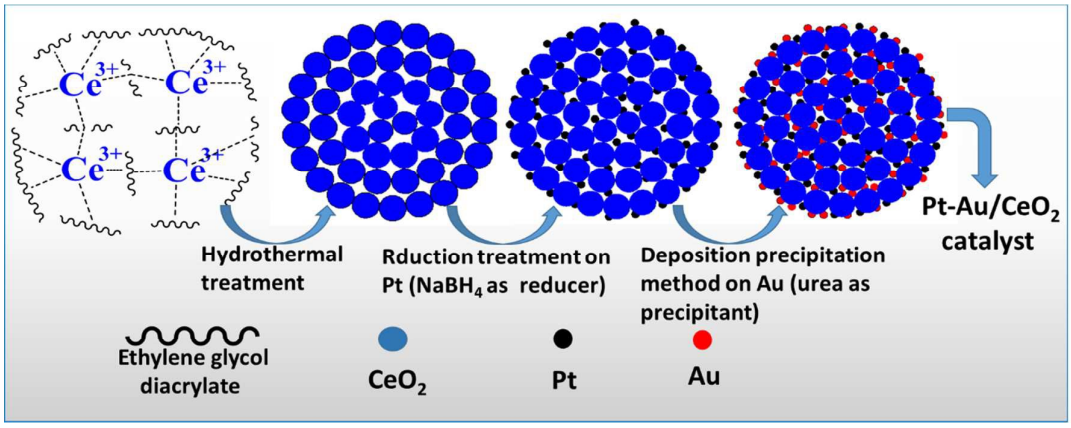

Fig. 1

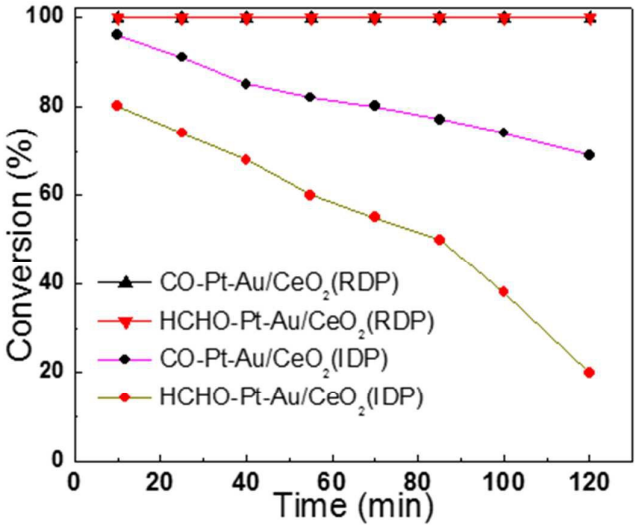

Fig. 2

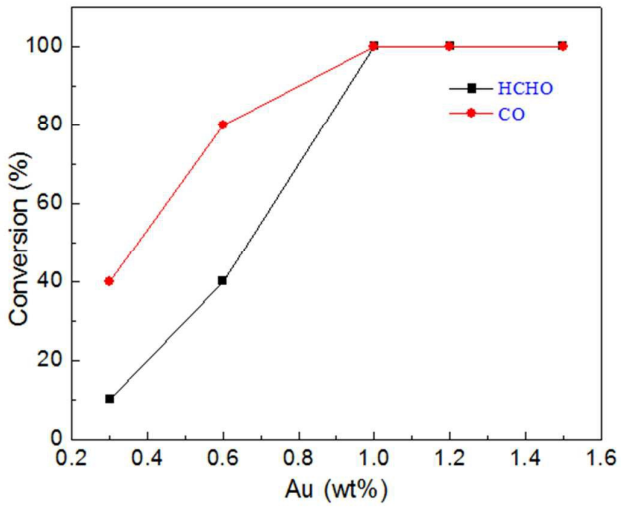

Fig. 3

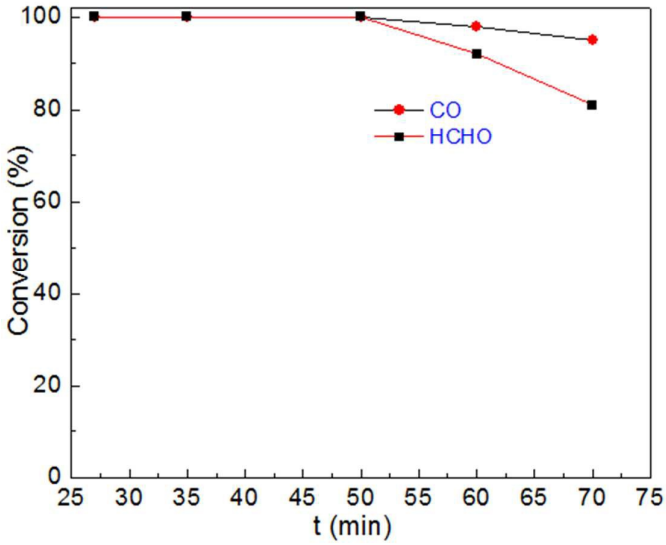

652

653 **Fig. 4**

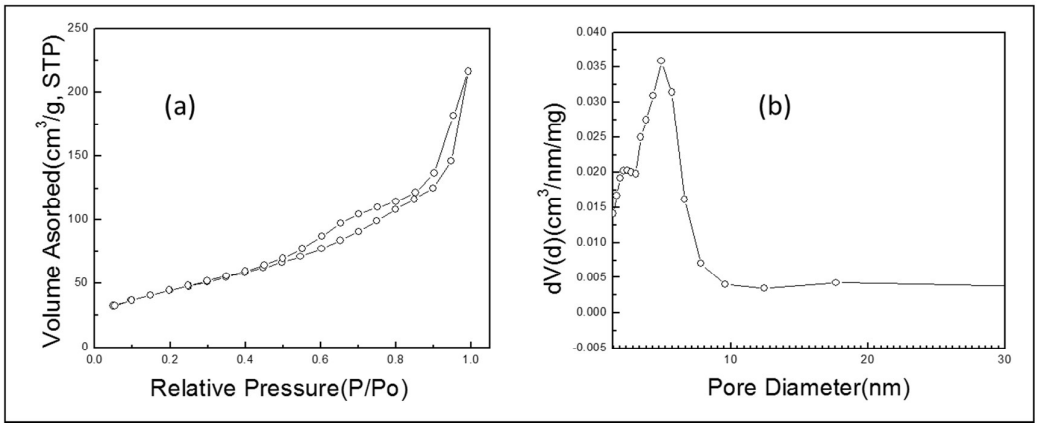

654

655

656

657

Fig. 5

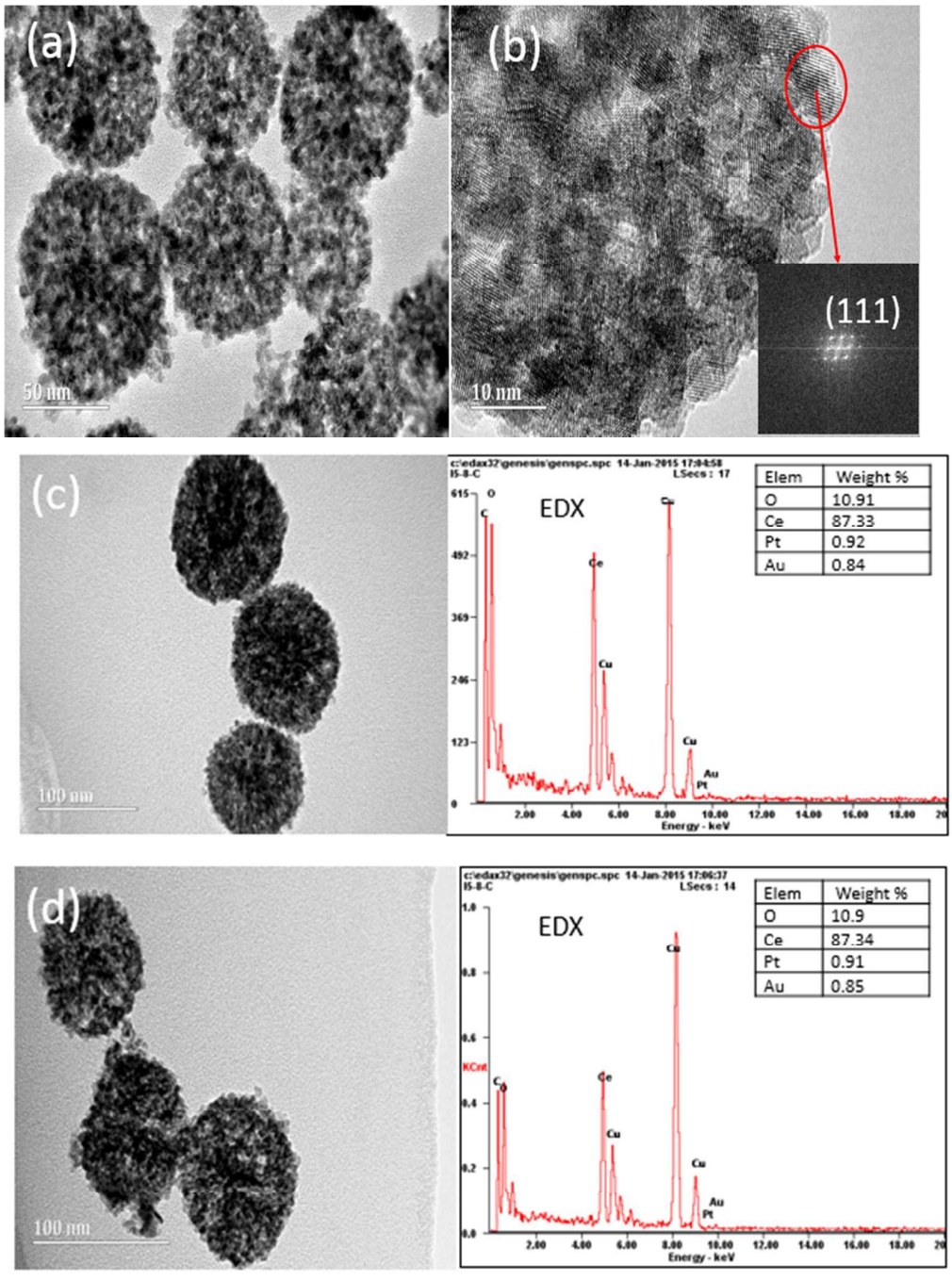

Fig. 6

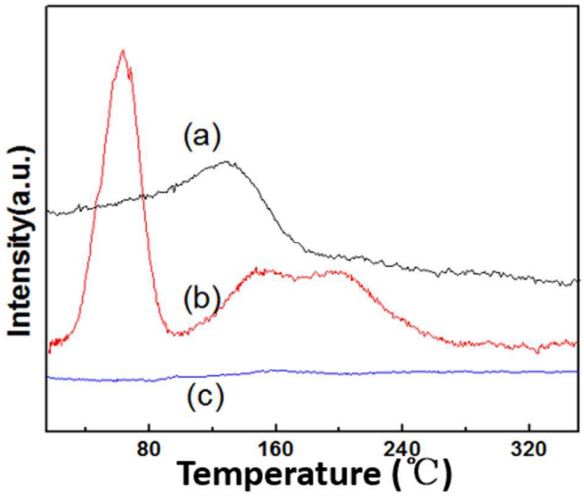

700 **Fig. 7**

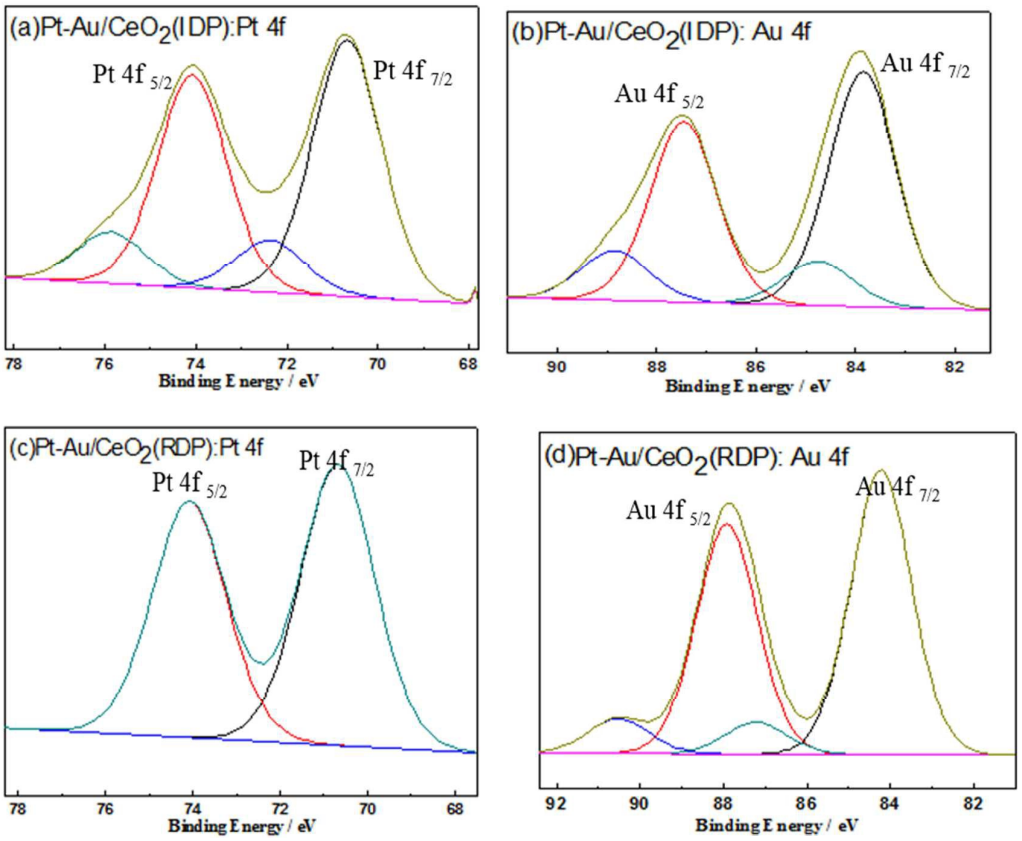

701

702

703

Fig. 8

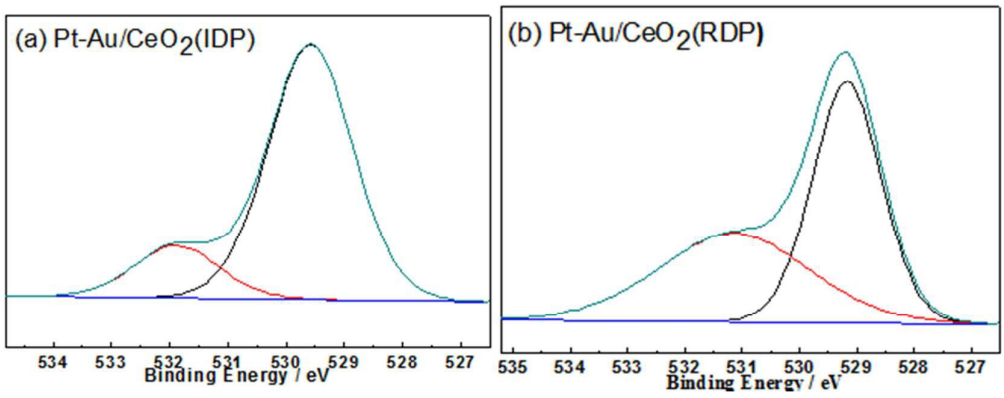

Fig. 9

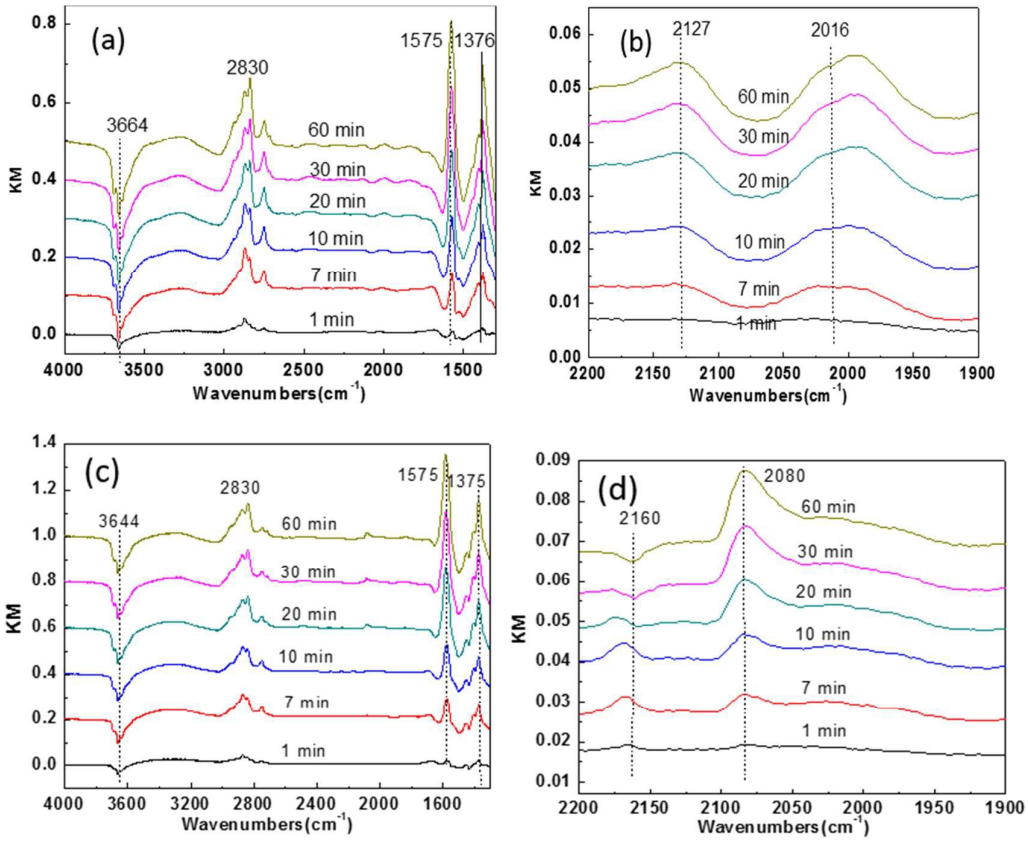

753

754 **Fig. 10**

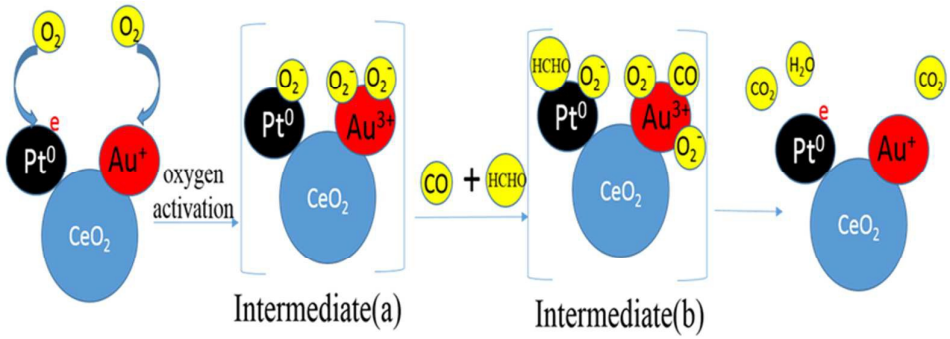

755

756